Low-Speed Magic-Angle-Spinning Carbon-13 NMR of Fruit Tissue

Qing Wen Ni and Thomas M. Eads*

Department of Food Science and Whistler Center for Carbohydrate Research, Purdue University, West Lafayette, Indiana 47907-1160

High-resolution carbon-13 NMR spectra of intact fruit tissues (grape, peach, persimmon, banana, and apple) were obtained while spinning the sample at the "magic angle" (MAS) to improve resolution. Only low speeds were required (a few hundred hertz) to reduce susceptibility broadening, which decreased as apple > banana > grape. Fructose, glucose, and sucrose resonances appeared with correct chemical shifts, thus permitting their identification and quantitation. The most abundant anomers of fructose and glucose were observed. Scalar ^{1}H–^{13}C couplings were observable as multiplets in spectra taken without proton decoupling, providing an aid to assignment. Measured values of nuclear Ovrhauser effect (NOE) and longitudinal relaxation time T_1 were consistent with rapid, effectively isotropic tumbling of sugar molecules, at rates very close to those observed in solutions of pure sugars. Potential applications of MAS NMR to fruit include quality assessment, analysis of chemical change accompanying ripening and senescence, and measuring the in situ physical state of dissolved components.

INTRODUCTION

Quantitative measures of quality play an important role in managing postharvest fruit quality and in assessing fruit as raw material for food and beverage processing (Kays, 1991). While many methods are in use, an interesting cluster of quality assessment methods based on nuclear magnetic resonance (NMR) is under development (Coombe and Jones, 1983; Chen et al., 1989; Cho and Krutz, 1989; Cho et al., 1991). NMR can be used to generate a signal from magnetically active nuclei such as ^{13}C and ^{1}H (proton) in molecules in liquid phases in fruit tissue.

Analysis of the time-decaying proton NMR signal has been proposed as the basis for quality assessment of whole fruit (Cho and Krutz, 1989). Both water and dissolved sugars, the two most abundant liquid-phase components, contribute to the ^{1}H signal, with water ^{1}H dominating. NMR can also be used to generate spectra from intact fruit tissue, in which identifiable peaks appear at the resonance frequencies of water or metabolite nuclei (Coombe and Jones, 1983; Cho et al., 1991). Narrow NMR peaks are expected, since the primary line-broadening interactions, namely internuclear magnetic dipolar interactions (^{1}H–^{1}H or ^{1}H–^{13}C), should be suppressed by fast molecular reorientation of sugar molecules in the aqueous phase. In fact, low molecular weight intracellular metabolites produce lines narrow enough for NMR studies of metabolism in intact plant tissue to become feasible. This has been demonstrated for ^{13}C, ^{15}N, and ^{31}P as observed nuclei (see the review by Martin, 1985). However, in the ^{1}H NMR work of Cho et al. (1991) with fruit tissue, sugars appeared as a broad, featureless envelope, indicating that resonance widths were greater than the separations between peaks. The widths were much greater than those observed in the same spectrometer on samples of sugars dissolved in water, i.e. about 1–2 Hz. The excess broadening was attributed primarily to magnetic susceptibility inhomogeneity, which is expected on theoretical grounds to occur in physically inhomogeneous substances (Doskocilova et al., 1975) and observed experimentally in other biological tissues (Rutar et al., 1988), emulsions (Eads et all, 1991), and foods (Eads, 1991; Eads, 1992).

* Author to whom correspondence should be addressed. Telephone: (317) 494-1749. Fax: (317) 494-7953.

In the work reported here, we have obtained ^{13}C NMR spectra in order to observe sugars in intact fruit tissue. Although this nucleus is inherently much less sensitive than ^{1}H, some advantages are realized. ^{13}C chemical shifts are spread over a 20-fold greater range than ^{1}H shifts; the broadening effect of magnetic susceptibility inhomogeneity is expected from theory (Doskocilova et al., 1975) to be about one-fourth that observed for ^{1}H spectra; and water does not interfere. Advantages of low-speed magic-angle spinning, including improved resolution and accuracy of chemical shifts, are also realized, enabling identification of sugars, approximate analysis of sugars, detection of anomers of fructose and glucose, measurement of scalar couplings (J_{CH}) between ^{1}H and ^{13}C nuclei connected by covalent bonds, measurement of nuclear Overhauser enhancement (NOE) values, measurement of ^{13}C longitudinal relaxation times (T_1), and analysis of molecular motions of dissolved sugars in situ. The nuclear Overhauser effect is also shown to provide a means of sensitivity enhancement.

MATERIALS AND METHODS

Sample Preparation. For magic-angle spinning experiments, a glass tube with the same inner diameter as the NMR rotor was pressed into the edible portion of the fresh fruit to cut a cylindrical plug which was then transferred to the rotor. The cylindrical zirconia rotor (7-mm o.d.; 0.8-mm wall thickness; 20-mm overall length) was sealed with caps equipped with tight-fitting O-rings. Sample length is about 9 mm, and volume is 0.35 mL. For conventional experiments, a cylindrical plug is cut to 11-mm diameter, 50-mm length, and gently put into a 12-mm o.d. glass NMR tube. A 5.7-mL sample is contained within the coil in the conventional probe. Fruit samples were purchased locally and used when ripe, as judged by the usual subjective criteria.

NMR Experiments. NMR spectra were acquired on a high-resolution NMR spectrometer (Nicolet NT 200) with 4.7 T superconducting magnet, upgraded as previously described (Wu et al., 1992). The operating frequency was 50.3 MHz for ^{13}C and 200 MHz for ^{1}H. For single-pulse ^{13}C experiments, a 7-μs pulse produced a 90° tip angle in the MAS probe, and a 23-μs 90° pulse was used for the conventional probe. Typical parameters include acquisition time of 0.256 s, sweep width 8 KHz, data size 12K points, and 7000 scans.

For proton-decoupled ^{13}C NMR spectra with no nuclear Overhauser enhancement (NOE), the proton decoupler is turned on during acquisition of the ^{13}C free induction decay (FID), but off during the relaxation delay (gated decoupling). The decoupler

0021-8561/92/1440-1507$03.00/0

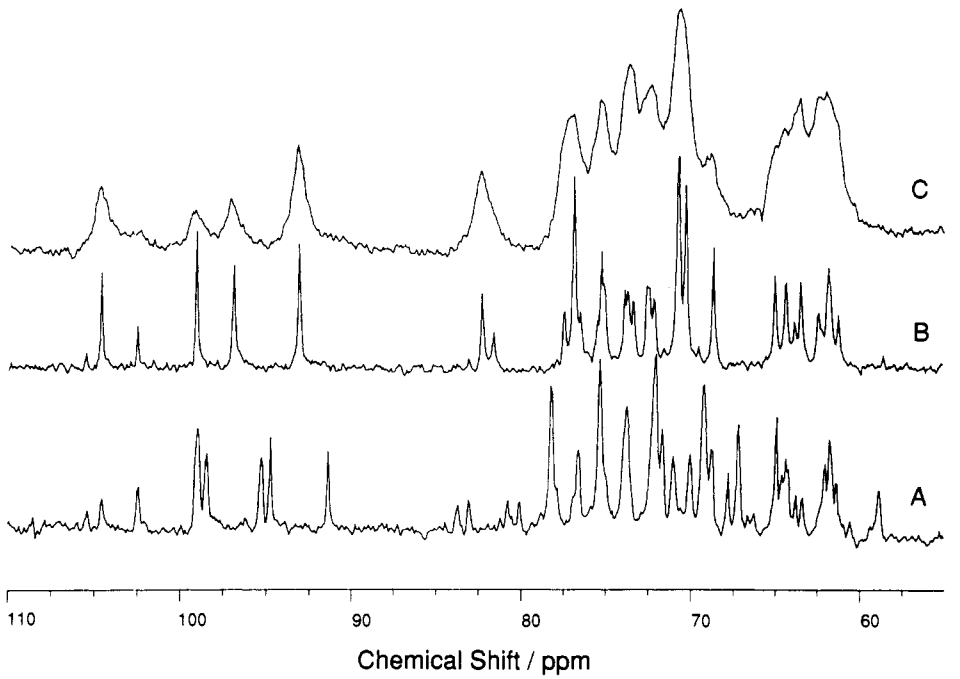

Figure 1. ^{13}C NMR (50 MHz) spectra of intact banana tissue: [effects of magic-angle spinning (MAS) and low power (scalar) proton decoupling]: (A) MAS spectrum obtained without decoupling; (B) MAS spectrum obtained with decoupling; (C) non-MAS spectrum obtained in a conventional high-resolution probe, with decoupling. Sample preparation and NMR method are described in the text. Vertical scaling adjusted for convenient display.

is left on during the relaxation delay for spectra with NOE. The WALTZ method of decoupling was employed (Shaka, 1983).

Sample temperature was maintained at 22 ± 1 °C. A two-channel probe (^1H decouple, ^{13}C observe) equipped for magic-angle spinning (Doty Scientific, Inc.) was used for MAS experiments; a conventional high-resolution two-channel probe (^1H, ^2H) was used otherwise.

For measurement of nuclear Overhauser enhancement (NOE), an "interleave" method was used, scans being alternately taken for NOE and non-NOE. In this method the decoupler is continuously on, but during gated decoupling (non NOE), the decoupler frequency is switched to be 1 MHz from the proton resonance frequency and therefore ineffective.

An inversion–recovery Fourier transform (IRFT) method (Vold et al., 1968) was used to measure the longitudinal relaxation time (T_1). Nine values of variable delay time (τ), ranging from 0.5 ms to 10 s were used to acquire a T_1 data set. Each glucose spectrum (τ) was acquired with 500 scans (banana, 2000 scans).

RESULTS AND DISCUSSION

Resolution Improvement by Magic-Angle Spinning. ^{13}C NMR spectra of intact ripe fruit tissue were obtained with and without MAS. For the MAS experiment, a probe equipped for magic-angle spinning was employed; for the non-MAS experiment, a conventional high-resolution probe (the tube axis parallel to the applied static field) was used. The results for banana are shown in Figure 1, in which the pattern of resonances is recognizable as that of a mixture common sugars. In the proton-decoupled non-MAS spectrum (Figure 1C) the line widths are about 80 Hz, which is broader than those observed in the proton-decoupled MAS spectrum (Figure 1B) by a factor of 10 or more. It is well established that by spinning the sample about an axis that makes the angle of 54° 44′ with the applied external field, at a spinning frequency greater than inhomogeneous broadening, such broadening can thereby be reduced (Andrew, 1971; Doskocilova et al., 1975; Rutar et al., 1988; Eads 1991; Eads et al., 1991). The full width at half height ($\Delta\nu_{1/2}$) of ^{13}C resonances ranges from 2.5 to 6 Hz in the MAS spectra of various fruit samples (Figure 1B and Figure 2). At least 26 peaks are distinguishable (Figure 1B), and their assignments are discussed below (Figure 4).

Scalar proton coupling is evident in the multiplet structure of ^{13}C resonances in MAS spectra obtained with no proton decoupling (Figure 1A). In the range of 80–100 ppm, the coupling constants (J_{CH}) of various carbons with single attached protons range from about 148 to 168 Hz, in agreement with previous observations (Wehrli et al., 1988). By application of low power, broad-band ^1H decoupling, collapse of the ^{13}C multiplets is effected, and the signal-to-noise ratio is improved. In the resulting spectrum (Figure 1B) most resolved peaks correspond to single, magnetically nonequivalent carbons.

Comparison of Spectra from Different Fruits. Proton-decoupled ^{13}C NMR spectra of grape, persimmon, banana and apple acquired in MAS and non-MAS experiments are compared in Figure 2. Line widths of ^{13}C resonances in non-MAS spectra of fresh fruits are obviously sample dependent. The differences correspond primarily to magnetic susceptibility inhomogeneity, not viscosity or exchange. This is shown by the similar effectiveness of line narrowing by MAS. Susceptibility inhomogeneity broadening is proportional to the difference between magnetic susceptibility of the liquid phase containing the observed nuclei and that of other phases nearby. In fruit, the relevant difference would be between cytoplasm (containing dissolved sugars) and cell walls, air cells, starch granules, vacuoles, etc. The maximum line broadening would occur when all of the liquid is contained in a thin shell around the domain of different susceptibility. In this case, the *maximum* broadening is approximated by $\Delta\nu \approx (8\pi/3)\,\Delta\chi\nu_L$, where $\Delta\chi$ is the difference between volume susceptibilities and ν_L is the Larmor frequency of the nucleus of interest in the liquid phase (Doskocilova et al., 1975). When not all the liquid is in a thin layer, there will be less broadening.

Resolution in the non-MAS spectrum from grape tissue approaches that of the MAS spectrum (Figure 2A). The line widths in the non-MAS and MAS spectra (data

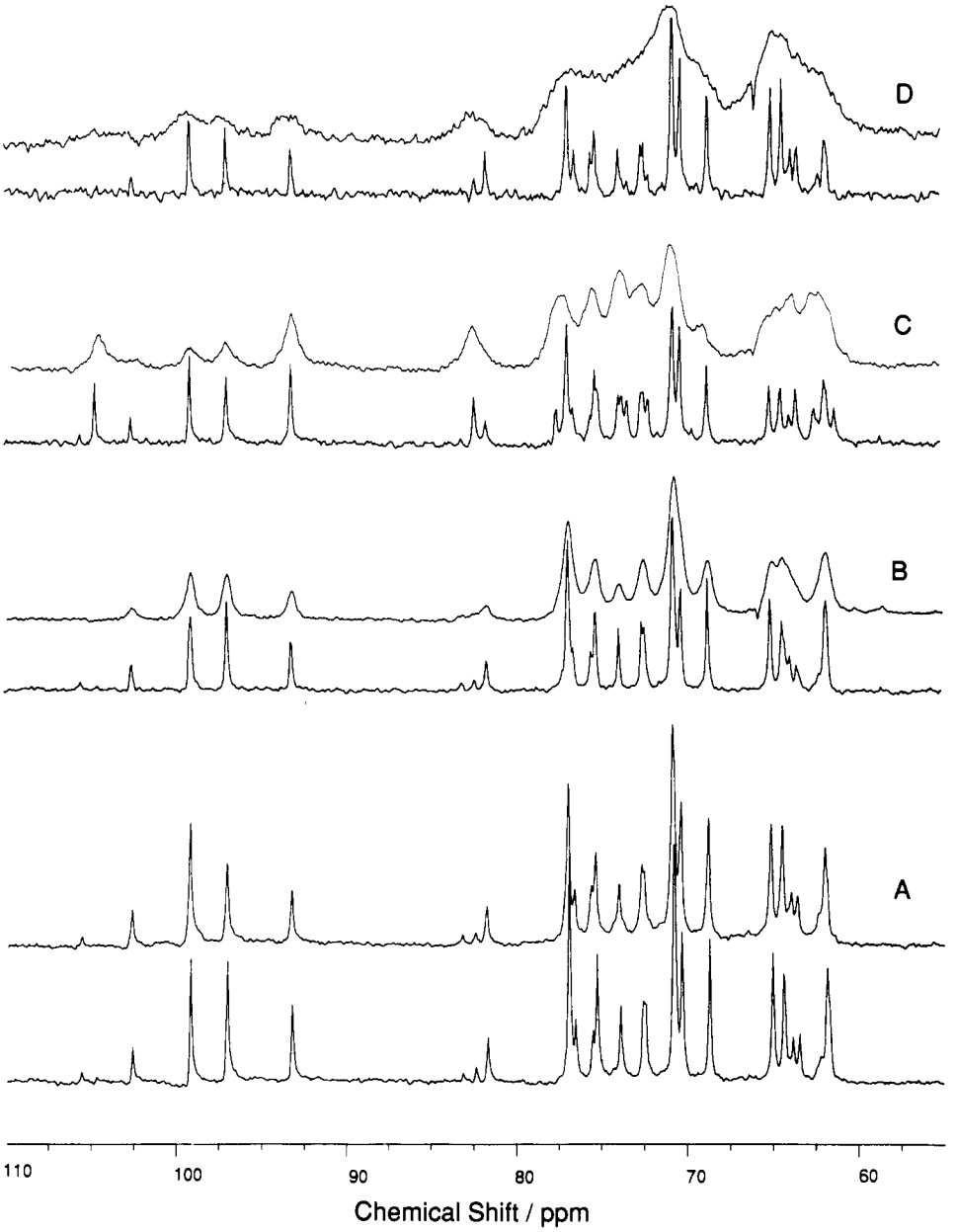

Figure 2. Proton scalar decoupled 50-MHz ^{13}C NMR spectra of intact fruit tissue (effect of magic-angle spinning shown in lower spectra: (A) grape; (B) persimmon; (C) banana; (D) apple. Vertical scaling adjusted for convenient display.

processed without line broadening) are about 4–7 Hz and 2.5–4 Hz, respectively. This is consistent with the microstructure of grape flesh, which has very large liquid-filled cells, nearly devoid of inclusions such as starch granules or air cells (Mohsenin, 1970). Thus susceptibility broadening is minimal for the grape sample.

At the other extreme, the non-MAS spectrum of apple (Figure 2D) shows a sample-dependent line width ranging from 100 to 150 Hz, suggesting that magnetic susceptibility effects are fairly large in this fruit and may vary among samples. The microstructure of apple tissue is also consistent with this interpretation, showing air voids in the tissue (Trakontivakorn et all, 1988) which also leads to a lower density than that calculated from chemical composition (Lewis, 1990). The magnetic susceptibility difference is greater between adjacent aqueous and air domains than between water and any other substance that might be found in fruit tissue. The maximum susceptibility broadening for an aqueous 20% solution of sugars surrounding an air cell is estimated using the formula above to be 313 Hz. (Values for volume susceptibilities were taken from Weast (1986); the value for χ(solution) was obtained by assuming that volume susceptibilities of water and sugars are additive.) This is larger than that observed, since the volume fraction of air is less than 30% in apple tissue (Trakontivakorn et al., 1988).

The broadenings in the spectra of our particular persimmon and banana samples are between those of grape and apple. Carbohydrate resonances broader than expected for aqueous solution have been observed previously in non-MAS ^{13}C NMR spectra of algae (Norton et al., 1982), xerophilic fungi (Hocking et al., 1983), and intact soybeans (Ishida et al., 1987). The origins of line broadening were not addressed in those studies.

The MAS line widths of all the fruit samples examined are in the range of 2.5–6 Hz. The values are close to the average value of 2 Hz obtained for the various resonances of pure glucose dissolved at 20 wt % in water, the spectrum being obtained in the MAS probe under the same conditions as used for fruit (data not shown). The difference may be due to several mechanisms, including incomplete removal of susceptibility broadening by MAS,

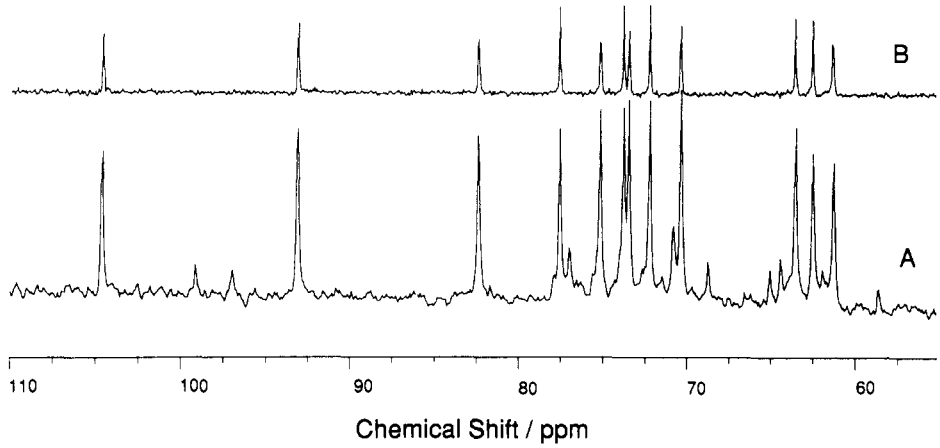

Figure 3. Proton scalar decoupled 50-MHz ^{13}C NMR spectra of (A) peach tissue (8000 scans) and (B) sucrose in water (1000 scans), each obtained with magic-angle spinning. Note exact correspondence of sucrose resonances in the two spectra. Vertical scaling adjusted for convenient display.

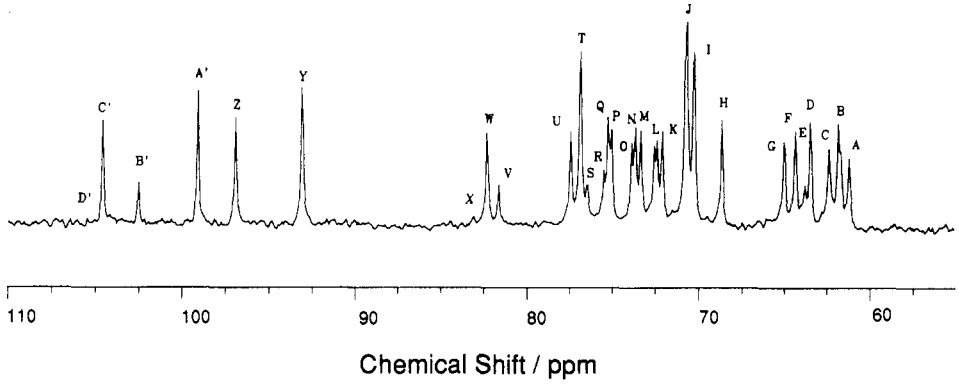

Figure 4. ^{13}C chemical shift assignments for the proton scalar decoupled MAS spectrum of banana tissue. The assignments are as follows: A, Suc C-6; B, Glu_p C-6; C, Suc C-1′; D, Suc C-6′; E, αFru_f C-1 and αFru_f C-6; F, βFru_p C-6; G, βFru_pC-1; H, βFru_p C-5; I, Suc C-4 and βFru_p C-3; J, αGlu_p C-5 and βFru_p C-4; K, Suc C-2; L, Glu_p C-4; M, Suc C-5; N, Suc C-3; O, Glu_p C-3; P, Suc C-4′; Q, Glu_p C-2; R, βFru_f C-3; S, βFru_f C-4; T, βGlu_p C-5; U, Suc C-3′; V, αFru_f C-3; W, Suc C-5′; X, αFru_f C-4; Y, Suc C-1 and αGlu_p C-1; Z, βGlu_p C-1; A′, βFru_p C-2; B′, βFru_f C-2; C′, Suc C-2′; D′, αFru_f C-2. The nomenclature for assignments is as follows: The sucrose ^{13}C resonances are labeled as Suc C-1 through Suc C-6 coresponding to the glucose portion of the sucrose molecule, and Suc C-1′ through Suc C-6′ for the fructose portion. The fructose ^{13}C resonances are labeled αFru_f C-1 through αFru_f C-6, βFru_f C-2 through βFru_f C-6, and βFru_p C-2 through βFru_p C-6 for the α-D-fructofuranose, β-D-fructofuranose, and β-D-fructopyranose respectively. Here, αGlc_p C-1 and $BGlc_p$ C-1, or αGlc_p C-5 and βGlc_p C-5 represent the C-1 or C-5 carbon of α-D-glucopyranose and β-D-glucopyranose, respectively. Glc_p C-2 to Glc_p C-4 and Glc_p C-6 represent the C-2, C-3, C-4, and C-6 carbons of either α-D-glucopyranose or β-D-glucopyranose, because these carbons have virtually identical chemical shifts in both anomers.

influence of paramagnetic species, temperature gradients with the sample, or incomplete motional averaging of internuclear dipolar interactions. The last mechanism seems improbable, as the T_1 and NOE suggest efficient motional averaging data (see below).

Identification of Fruit Sugars and Resonance Assignments. The relative values of chemical shifts observed within a MAS spectrum are identical to those obtained in sugar–water system, since MAS eliminates the need to correct for internal susceptibility effects on shift (Garroway, 1982; Rutar et al., 1988). As an example, the chemical shifts of dominant peaks in the proton-decoupled MAS ^{13}C NMR spectrum of peach tissue exactly match those of sucrose dissolved in water (Figure 3). Small peaks which match those of glucose and fructose can also be found in the peach spectrum. Thus, direct comparison may be made between MAS spectra and spectra given in "NMR libraries", which are obtained on homogeneous liquid samples in conventional NMR probes.

An example of chemical shift assignment is illustrated in Figure 4, for the proton-decoupled MAS spectrum of banana tissue. Chemical shifts of glucose, sucrose, and fructose carbon atoms were previously determined (Angyal, 1965; Angyal et al., 1976; Rosenthal et al., 1976; Bock, 1982). The assignments indicated in Figure 4 were made by superimposing MAS spectra of D-glucose (not shown), D-sucrose (Figure 3B), and D-fructose (not shown) dissolved in water.

It is important to note that a D-fructose solution contains an equilibrium mixture of its anomers of β-D-fructopyranose, β-D-fructofuranose, and α-D-fructofuranose. The proportion of anomers would depend on temperature, and at room temperature, the proportion is expected to be 18.6:4.8:1 (Shallenberger, 1982). We observed all three anomers in the MAS spectrum of pure fructose. The banana spectrum contains most of peaks expected, although the current signal to noise ratio does not permit a reliable estimate of their ratios. Similarly, at room temperature, an aqueous solution of glucose will be an equilibrium mixture of α-D-glucopyranose, β-D-glucopyranose, α-D-glucofuranose, β-D-glucofuranose, and the *gem*-diol tautomer, present in the proportions of 38.8, 60.9, 0.14, 0.15, and 0.0045, respectively (Maple et al., 1987). Of these, resonances for all but the *gem*-diol are observable in the ^{13}C MAS spectrum of pure glucose in water (not shown). The banana spectrum contains resonances of α-D-glucopyranose and β-D-glucopyranose. It is clear that fructose and glucose in intact banana tissue exist as a mixture of their anomers. A similar result is obtained for all other

Table I. Weight Ratios of Sugars Determined by ^{13}C NMR of Single Samples of Intact Tissues of Various Fruits

	ratio[a] (rel to sucrose)			
	glucose[b]		fructose[c]	
fruit	obs	ref	obs	ref
apple	2.08	0.31[d]	3.25	1.60[d]
grape	6.13	4.05[d]	6.46	4.03[d]
banana	1.05	0.61[e]	1.19	0.69[e]
peach	0.10	0.13[d]	0.12	0.17[d]
persimmon	4.57	*f*	4.96	*f*

[a] Single determinations, calculated from integrals of peaks at indicated positions in ^{13}C NMR spectra (see text for method). [b] Based on integration of the peak at 96.8 ppm, belonging to βGlu_p C-1. [c] Based on integration of the peak at 102.6 ppm, belonging to βFru_f C-2. [d] Ockerman, H. W. *Food Science Sourcebook*, 2nd ed.; Van Nostrand Reinhold: New York, 1991; Part 2, p 1368. [e] Ensminger, A. H.; Ensminger, M. E. *Foods & Nutrition Encyclopedia*, 1st ed.; Pegus Press: Clovis, CA, 1983; Vol. 1, p 341. [f] Not available.

fruit samples whose spectra were obtained with an adequate signal-to-noise ratio.

Comparison among the MAS spectra of fruits shows differences in their sugar compositions (Figure 2). In addition, differences occur among samples from individual pieces of fruit of a single variety.

Quantitative Analysis. Relative amounts of sugars in a sample of fruit tissue may be determined by integration of resonances. The experimental requirements for detecting all peaks with equal efficiency have been specified previously (Martin et al., 1980) and are satisfied in the experiments reported here.

It is usually possible to identify at least one unique resonance for each analyte present. Sugar concentration in the fruit is then obtained from the relation

$$c_{i,fruit} = I_{i,fruit}(\delta)c_{i,std}/I_{i,std}(\delta) \quad (1)$$

where $c_{i,fruit}$ is the concentration of sugar i, $c_{i,std}$ is the concentration of sugar i, a standard sample, $I_{i,fruit}(\delta)$ is the integral of the analyte peak at chemical shift position δ in the fruit sample, and $I_{i,std}(\delta)$ is the integral of the corresponding peak in the standard sample spectrum, obtained under identical conditions. If the signal-to-noise ratio is good, single resonances of particular sugars will suffice. (Alternatively, each I_i may be the sum of any number of identifiable peaks for that sugar, as long as the number of carbon atoms is taken into account.)

A complication arises when the most convenient chosen peak corresponds to a magnetically inequivalent isomer. An example would be the C-1 carbons of glucose (αGlu_p C-1, 93.0 ppm; βGlu_p C-1, 96.8 ppm), only one of which can be integrated in the complex fruit spectrum. In such case, a value for I_i corresponding to the entire integral for that sugar may be obtained from the formula

$$I_i = I_{i,fruit}(\delta)I_{i,std}/I_{i,std}(\delta) \quad (2)$$

where $I_{i,std}$ is the total integral for the spectrum of a standard sample of the sugar i and $I_{i,std}(\delta)$ is the integral of the peak at the chemical shift position δ. The spectrum of the standard need not be obtained in the same NMR session as the spectrum of fruit. The ratios of values of I_i then give the desired result. The implicit assumption in this approach is that the position of anomeric equilibrium is the same in the fruit and standard.

The ratios of glucose and fructose to sucrose, obtained by the above method from the low-speed MAS ^{13}C NMR spectra of apple, grape, banana, peach, and persimmon are presented in Table I. The values are compared to those given in some compiled sources. The agreement is fair for all samples but apple, in which glucose and fructose are high relative to sucrose. This may be due to conversion of sucrose during storage and handling. A fresh apple was not tested. The results in Table I establish that the NMR method can be used for quantitation without isolation and separation of sugars. However, the precision of the method has not yet been determined, and a direct comparison between NMR results and standard chemical on the NMR samples was not attempted. Further work would be required to establish factors accounting for variance in sugar composition, such as botanical variety, geographical location, differences between individual pieces from the same harvest, ripeness, and prior storage conditions, or treatments. Such methods as principal component analysis might also be used to analyze fruit NMR spectra which are rich in detail and pattern.

Nuclear Overhauser Enhancement (NOE) and Sensitivity Enhancement. ^{13}C NOEs were measured during magic-angle spinning, using the interleave method (see Materials and Methods); results are shown in Figure 5. Observed NOE values ranged from 2.1 to 2.5 for individual ^{13}C resonances. The values are high, suggesting that ^{13}C nuclear relaxation is dominated by ^{13}C–^{1}H dipolar interaction (Lyerla et al., 1971). The nonminimum NOE value of each carbon is consistent with average molecular rotational correlation time shorter than about 6.4×10^{-11} s. This is discussed further in the next section. While the sensitivity gain is a benefit for detection, it affects individual resonances differently. Therefore, integrals of ^{13}C resonances in spectra obtained with enhancement would not provide accurate ratios of sugars.

^{13}C Longitudinal Relaxation (T_1) and Molecular Mobility. The ^{13}C longitudinal relaxation times T_1 of 20 wt % glucose solution and of glucose in banana were measured during MAS by the inversion–recovery method. The results are presented in Table II. T_1 values for glucose resonances in intact banana tissue are similar to those for the 20 wt % aqueous solution of pure glucose. Since T_1 is a sensitive function of molecular motion, the results suggest that rotational molecular mobility of glucose in banana is similar to that of pure glucose in 20% solution. The similarity of results for the second and third bananas gives rough indication of the precision of T_1 measurements on intact fruit. The second and third bananas come from the same bunch, and measurements were made within 18 h of each other.

In analyzing ^{13}C spin–lattice relaxation in sugars, two likely relaxation mechanisms must be considered, namely the chemical shift interaction and the ^{13}C–^{1}H dipole–dipole interaction (Abragam, 1961). The observed T_1 then may be written as

$$1/T_1^{OBS} = 1/T_1^{DD} + 1/T_1^{CS} \quad (3)$$

The values of $1/T_1^{DD}$ and $1/T_1^{CS}$ were estimated, at the field strength of these experiments, using values of 1.09 Å for internuclear distance r_{CH} (Cutsche and Pasto, 1975) and 30 ppm for the chemical shift anisotropy ($\sigma_\parallel - \sigma_\perp$) (Duncan, 1990) as required for the calculation. The chemical shift term was found to contribute only about 1% to the observed T_1 of carbohydrate resonances. Thus, longitudinal relaxation is dominated by the dipolar mechanism. This result can also be deduced from the result of the nuclear Overhauser enhancement measurement (Allerhand et al., 1971).

For molecules which exhibit effectively isotropic reorientation, and in which long-range ^{13}C–^{1}H interactions can be neglected, it will be (Solomon, 1955)

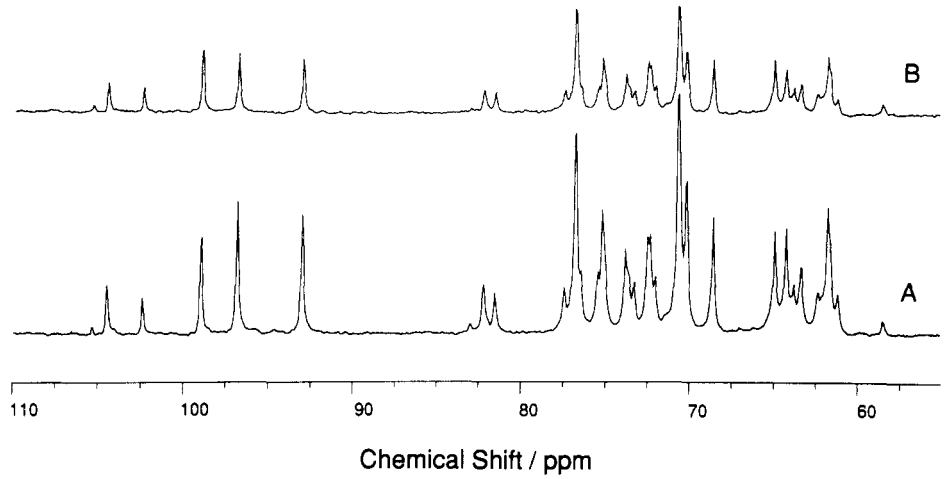

Figure 5. Nuclear Overhauser effect in the proton scalar decoupled 50-MHz ^{13}C NMR spectrum of intact banana tissue, obtained with the interleave method while spinning the sample at the magic angle (see Materials and Methods): (A) with enhancement and (B) without enhancement. A total of 8000 scans were acquired for each; vertical scaling is the same for each spectrum.

Table II. ^{13}C T_1 Relaxation Times of Glucose in Aqueous Solution and in Intact Banana Tissue

	T_1,[c] s							
sample	αC-1	βC-1	C-2	C-3	C-4	αC-5	βC-5	C-6
solution[a]	0.785	0.784	0.803	0.781	0.767	0.763	0.782	0.387
banana[b]	0.73	0.60	0.75	0.65	0.75	0.74	0.82	0.43
	0.57	0.44	0.52	0.52	0.59	0.53	0.56	0.22
	0.56	0.43	0.52	0.55	0.49	0.52	0.50	0.24

[a] 20 wt % glucose in water, the average of three separate measurements is given. [b] Edible portion of ripe fruit was used; results for three different bananas are given. The second and third bananas were from the same bunch, within 18 h of each other. [c] Only resonances from αGlc_p and βGlc_p were used. T_1's of ^{13}C were measured during magic-angle spinning at 300 Hz by the inversion–recovery method (see text for details) at 22 °C. The uncertainties in measured values of T_1 for glucose solution individual peaks are, for C-6, ±0.001 s (SD, n = 3) and, for other carbons, from ±0.0001 to ±0.003 s.

$$1/T_1^{DD} = \hbar^2\gamma_H^2\gamma_C^2 N r_{CH}^{-6}\tau_c \quad (4)$$

Here N is the number of directly attached protons, $\hbar$ = Planck's constant/2π, γ_H and γ_C are the gyromagnetic ratios for ^1H and ^{13}C, respectively, r_{CH} is the internuclear separation, and τ_C is the molecular rotational correlation time. From this equation it is evident that carbon C-6 will have a shorter T_1, because it has two attached protons. The other carbons have one attached proton.

By using eq 4, τ_C was calculated from the experimental values of T_1 (Table II). For this purpose, it was convenient to take the average NT_1 for the six carbons of glucose. The resulting correlation time of glucose in water is 64 ps. The estimates of τ_C for glucose in three separate bananas are 68, 95, and 98 ps, respectively. It is possible that the differences between glucose solution and banana, and between the first and second two bananas, may be associated with differences in viscosity, since the rotational correlation time is proportional to viscosity. Similar results for τ_C are expected for sugars in other ripe fruits with high water contents, while longer correlation times are expected for fruits with lower water content. Rotational motion of certain osmoregulatory low molecular weight carbohydrate metabolites in cells was previously found to be slightly more restricted than in pure solution as measured by ^{13}C T_1 relaxation (Norton et al., 1982; Hocking and Norton, 1983).

Minimum Magic-Angle Spinning Speed. The minimum spinning rate would be that which generates the least centrifugal force, thereby reducing stress on the sample, while reducing susceptibility broadening and removing spinning side bands from the spectral region of interest (Eads et al., 1991). After spinning fruit sample at kilohertz rates, separation of air, liquid, and solid was sometimes observed, whereas after spinning at a few hundred hertz, samples appeared to be unperturbed. The other strategies for minimizing centrifugal stress include reduced rotor diameter, lower field strength, and choice of observation of nuclei with smaller nuclear gyromagnetic ratio γ. Each method has its limits and may involve tradeoffs in sensitivity and selectivity.

For apple tissue spun between 300 and 1000 Hz, the line widths were all the same (data not shown). Indeed, at the lowest stable spinning speed of 300 Hz, the susceptibility broadening of 100–150 Hz seen in the non-MAS spectrum (Figure 2D, top) should already be removed. The minimum rate would be expected to be considerably less for the other fruits. This point will be particularly important in NMR analyses at low field, when using large volume MAS rotors (Zhang and Maciel, 1990), and for tissues that are more delicate.

Conclusions. A considerable advantage of ^{13}C NMR spectroscopy for analysis is the inherent selectivity that comes from the large range in chemical shifts. Realizing this advantage requires high resolution and accuracy of chemical shifts, both obtainable by using MAS. With appropriate care, the current method is capable of detecting species including sugar anomers in concentrations at least as low as 0.5%, although this may be inconvenient for routine analysis. Inverse ^{13}C detection via protons could further improve sensitivity (Martin and Crouch, 1991). The NMR approach could be extended to study chemical changes during ripening, senescence, dehydration, response to stress, etc. Physical information, such as changes of molecular mobility accompanying such processes, could also be measured. The substantial gain in resolution by MAS should permit application of multidimensional NMR in order to remove overlap of resonances, to probe molecular conformation in situ, to edit spectra, and to realize sensitivity gains. The methods described here are well-defined and general; they can be applied to other multiphasic, liquid-containing agricultural, food, and nonbiological materials.

ACKNOWLEDGMENT

This is paper number 13329 from the Indiana Agricultural Experiment Station, West Lafayette, IN. The financial assistance of the Whistler Center for Carbohydrate Research; Nestec, Ltd., Lausanne, Switzerland; and

ATI Instruments, Oak Park, IL, is gratefully acknowledged. We appreciate the contributions of P. Pellechia and R. Santini (Purdue) in Nicolet NT200 NMR spectrometer upgrade design and execution.

LITERATURE CITED

Abragam, A. *The Principles of Nuclear Magnetism*; Oxford University Press: London, 1961; p 61.

Allerhand, A.; Doddrell, D.; Komoroski, R. Natural Abundance Carbon-13 Partially Relaxed Fourier Transform Nuclear Magnetic Resonance Spectra of Complex Molecules. *J. Chem. Phys.* **1971**, *55*, 189–198.

Andrew, E. R. The Narrowing of NMR Spectra of Solids by High Speed Specimen Rotation and the Resolution of Chemical Shift and Spin Multiplet Structure for Solids. *Prog. NMR Spectrosc.* **1971**, *8*, 1–39.

Angyal, S. J. Conformational Analysis in Carbohydrate Chemistry. In *Conformational Analysis*; Eliel, E. L. et al., Eds.; Interscience: New York, 1965.

Angyal, S. J.; Bethell, G. S. Conformational Analysis in Carbohydrate Chemistry. III The ^{13}C N.M.R. Spectra of the Hexuloses. *Aust. J. Chem.* **1976**, *29*, 1249–1265.

Bock, K. The Conformational Properties of Sucrose in Aqueous Solution: Intramolecular Hydrogen-Bonding. *Carbohydr. Res.* **1982**, *100*, 63–74.

Chen, P.; McCarthy, M. J.; Kauten, R. NMR for Internal Quality Evaluation of Fruits and Vegetables. *Am. Soc. Agric. Eng.* **1989**, *32*, 1747–1753.

Cho, S. I.; Krutz, G. W. Fruit Ripeness Detection by Using NMR. *ASAE Publ.* **1989**, paper 89-6620.

Cho, S. I.; Bellon, V.; Eads, T. M.; Stroshine, R. L.; Krutz, G. W. Sugar Content Measurement in Fruit Tissue Using Water Peak Suppression in High Resolution ^{1}H Magnetic Resonance. *J. Food Sci.* **1991**, *56*, 1091–1094.

Coombe, B. G.; Jones, G. P. Measurement of the Changes in the Composition of Developing Undetached Grape Berries by Using ^{13}C NMR Techniques. *Phytochemistry* **1983**, *22*, 2185–2187.

Cutsche, C. D.; Pasto, D. J. *Fundamentals of Organic Chemistry*; Prentice-Hall: Englewood Cliffs, NJ, 1975; p 45.

Doskocilova, D.; Tao, D. D.; Schneider, B. Effect of Macroscopic Spinning Upon Linewidth of NMR Signals of Liquid in Magntically Inhomogeneous System. *Czech. J. Phys.* **1975**, *B25*, 202–209.

Duncan, T. *A Compilation of Chemical Shift Anisotropies*; Farragut Press: Chicago, 1990; p C-20.

Eads, T. M. Multinuclear High Resolution and Wide Line NMR Methods for Analysis of Lipids. In *Analyses of Fats, Oils and Lipoproteins*; E. G. Perkins, Ed.; American Oil Chemists' Society: Champaign, IL, 1991.

Eads, T. M. New Strategies for Measuring Molecular Structural Dynamics, and Composition of Food Materials by NMR. In *Frontiers in Carbohydrate Research-2*; Chandrasekaran, R., Ed.; Elsevier: New York, 1992.

Eads, T. M.; Weiler, R. K.; Gaonkar, A. G. Detection of Water in the Internal Aqueous Phase of W/O/W Multiple Emulsions Using Magic Angle Spinning Proton NMR. *J. Colloid Interface Sci.* **1991**, *145*, 466–77.

Garroway, A. N. Magic Angle Sample Spinning of Liquids. *J. Magn. Reson.* **1982**, *49*, 168.

Hocking, A. D.; Norton, R. S. Natural-abundant ^{13}C Nuclear Magnetic Resonance Studies on the Internal Solutes of Xerophilic Fungi. *J. Gen. Microbiol.* **1983**, *129*, 2915–2925.

Ishida, N.; Kano, H.; Kobayashi, T. Estimation of Biological Activities by NMR in Soybean Seeds during Maturation. *Agric. Biol. Chem.* **1987**, *51*, 301–307.

Kays, S. J. *Postharvest Physiology of Perishable Plant Products*; Van Nostrand Reinhold: New York, 1991; p 145.

Lewis, M. J. *Physical Properties of Foods and Food Processing System*; Ellis Horwood: London, 1990; p 54.

Lyerla, J. R.; Grant, D. M.; Harris, R. K. Dipolar Contributions to Carbon-13 Relaxation Times. *J. Phys. Chem.* **1971**, *75*, 585–588.

Maple, S. R.; Allerhand, A. Detailed Tautomeric Equilibrium of Aqueous D-Glucose: Obsrevation of Six Tautomers by Ultrahigh Resolution Carbon-13 NMR. *J. Am. Chem. Soc.* **1987**, *109*, 3168–3169.

Martin, F. Monitoring Plant Metabolism by ^{13}C, ^{15}N, and ^{14}N Nuclear Magnetic Resonance Spectroscopy. A Review of the Applications to Algae, Fungi and Higher Plants. *Physiol. Veg.* **1985**, *23*, 463–490.

Martin, G. E.; Crouch, R. C. Inverse-Detected Two-Dimensional NMR Methods: Applications in Natural Products Chemistry. *J. Nat. Prod.* **1991**, 1–70.

Martin, M. L.; Martin, G. L.; Delpuech, J. *Practical NMR Spectroscopy*; Heyden: Philadelphia, PA, 1980; pp 350–376.

Mohsenin, N. N. *Physical Properties of Plant and Animal Materials*; Gordon and Breach Science Publishers: New York, 1970; pp 15–54.

Norton, R. S.; Mac, M. A.; Borotwitzka, L. J. The physical State of Osmoregulatory Solutes in Unicellular Algae. *Biochem. J.* **1982**, *202*, 699–706.

Rosenthal, S. N.; Fendler, J. H. ^{13}C NMR Spectroscopy in Macromolecular Systems of Biochemical Interest. *Adv. Phys. Org. Chem.* **1976**, *13*, 279–424.

Rutar, V.; Kovac, M.; Lahajnar, G. Improved NMR Spectra of Liquid Components in Heterogenous Samples. *J. Magn. Reson.* **1988**, *80*, 133–138.

Shaka, A. J.; Keeler, J.; Freeman, R. Evaluation of a New Broadband Decoupling Sequence: WALTZ-16. *J. Magn. Reson.* **1983**, *53*, 313–340.

Shallenberger, R. S. *Advanced Sugar Chemistry*; Saybrook Press: Saybrook, CT, 1982; p 196.

Solomon, I. Relaxation Processes in a System of Two Spins. *Phys. Rev.* **1955**, *99*, 559–565.

Trakontivakorn, G.; Patterson, M. E.; Swanson, B. G. Scanning Electron Microscopy of Cellular Structure of Granny Smith and Red Delicious Apples. *Food Microstruct.* **1988**, *7*, 205–212.

Vold, R. L.; Waugh, J. S.; Klein, M. P.; Phelps, D. E. Measurement of Spin Relaxation in Complex System. *J. Chem. Phys.* **1968**, *48*, 3831–3832.

Weast, R. C., Ed. *CRC Handbook of Chemistry and Physics*, 66th ed.; CRC Press: Boca Raton, FL, 1986; p E122.

Wehrli, F. W.; Marchand, A. P.; Wehrli, S. *Interpretation of Carbon-13 NMR Spectra*; Wiley: New York, 1988; pp 211–240.

Wu, J. Y.; Bryant, R. G.; Eads, T. M. Detection of Solid-Like Components in Starch Using Cross-Relaxation and Fourier Transform Wide Line ^{1}H NMR Methods. *J. Agric. Food Chem.* **1992**, *40*, 449–455.

Zhang, M.; Maciel, G. E. Enhanced Signal-to-Noise Ratios in the Nuclear Magnetic Resonance Analysis of Solids, Using Large-Sample Magic-Angle Spinners. *Anal. Chem.* **1990**, *62*, 633–638.

Received for review January 31, 1992. Revised manuscript received June 15, 1992. Accepted June 19, 1992.

Registry No. Fructose, 57-48-7; glucose, 50-99-7; sucrose, 57-50-1; α-D-glucopyranose, 492-62-6; β-D-glucopyranose, 492-61-5; α-D-fructofuranose, 10489-79-9; β-D-fructofuranose, 470-23-5; β-D-fructopyranose, 7660-25-5.